Article

PERCEPTION

Perception
2017, Vol. 46(1) 50–77

DOI: 10.1177/0301006616672577
journals.sagepub.com/home/pec
SAGE

A Common Mechanism for Perceptual Reversals in Motion-Induced Blindness, the Troxler Effect, and Perceptual Filling-In

Dina Devyatko
National Research University Higher School of Economics, Moscow, Russia; Institute of Information Processing and Decision Making, University of Haifa, Israel

L. Gregory Appelbaum
Department of Psychiatry and Behavioral Sciences, Duke University School of Medicine, Durham, NC, USA

Stephen R. Mitroff
Department of Psychology, The George Washington University, Washington, DC, USA

Abstract
Several striking visual phenomena involve a physically present stimulus that alternates between being perceived and being "invisible." For example, motion-induced blindness, the Troxler effect, and perceptual filling-in all consist of subjective alternations where an item repeatedly changes from being seen to unseen. In the present study, we explored whether these three specific visual phenomena share any commonalities in their alternation rates and patterns to better understand the mechanisms of each. Data from 69 individuals revealed moderate to strong correlations across the three phenomena for the number of perceptual disappearances and the accumulated duration of the disappearances. Importantly, these effects were not correlated with eye movement patterns (saccades) assessed through eye tracking, differences in motion sensitivity as indexed by dot coherence and speed perception thresholds, or simple reaction time abilities. Principal component analyses revealed a single component that explained 67% of the variance for the number of perceptual reversals and 60% for the accumulated duration of the disappearances. The temporal dynamics of illusory disappearances was also compared for each phenomenon, and normalized durations of disappearances were well fit by a gamma distribution with similar shape parameters for each phenomenon, suggesting that they may be driven by a single oscillatory mechanism.

Corresponding author:
Dina Devyatko, Laboratory for Cognitive Research, National Research University Higher School of Economics, 46B Volgogradski prospekt, Moscow 109316, Russia.
Email: tsukit86@gmail.com

Keywords
motion-induced blindness, Troxler effect, perceptual filling-in, common timing mechanism, gamma approximation

Introduction

Psychologists have long benefited from studying multistable phenomena, wherein more than one possible percept can arise from a single stimulus. Ambiguous images, such as Jastrow's (1899) Duck-Rabbit and the Rubin's (1915) face-vase illusion, offer exciting demonstrations and draw broad public interest (e.g., Brugger & Brugger, 1993; Wiseman, Watt, Gilhooly, & Georgiou, 2011), while also serving as powerful research tools (e.g., Pitts, Martínez, Stalmaster, Nerger, & Hillyard, 2009; Pitts, Nerger, & Davis, 2007). By understanding the nature of how such multistable percepts alternate, it is possible to gain insight into the underlying mechanisms of perception and cognition. Studying the pattern of reversals between competing multistable percepts provides a tangible means to uncover the mechanisms of inhibition, adaptation, and attention that shape the content of human consciousness and have featured prominently in cognitive neuroscience in the last two decades or so (e.g., Blake, 2001; Chong & Blake, 2006; Leopold & Logothetis, 1999; Meng & Tong, 2004; Panagiotaropoulos, Deco, Kapoor, & Logothetis, 2012; Panagiotaropoulos, Kapoor, Logothetis, & Deco, 2013; Parkkonen, Andersson, Hämäläinen, & Hari, 2008; Srinivasan, Russell, Edelman, & Tononi, 1999; Tong, Meng, & Blake, 2006). Moreover, perceptual alternations have contributed to clarifying the link between visual awareness and oscillatory brain activity (Matsuzaki, Juhász, & Asano, 2012; Sokoliuk & VanRullen, 2013) which is thought to be responsible for the temporal structure of conscious perception (Jensen, Bonnefond, & VanRullen, 2012).

Competition for perceptual dominance can take many forms: alternations between stimulus interpretations (e.g., Necker cube), alternations between monocularly presented images (e.g., binocular rivalry), and alternations in visibility (e.g., motion-induced blindness [MIB]). ''Illusory disappearances''—wherein conscious percepts alternate between seeing an object and not seeing it—constitute a specific class of multistable phenomena that offer an excellent tool for studying visual awareness and the neural correlates of consciousness. These types of stimuli are especially useful in that they allow one to contrast neural activation associated with conscious perception and activation that is not accompanied by conscious perception for the same physical stimulus (Kim & Blake, 2005). For instance, binocular flash suppression and MIB have been used to examine activation in prefrontal cortex during perceptual transitions between visible and invisible states of the same physical stimulus (Libedinsky & Livingstone, 2011; Panagiotaropoulos et al., 2012), thereby revealing fundamental aspects of how neural activity relates to conscious perception.

Types and Theories of Illusory Disappearances

There are a variety of forms of illusory disappearances that have been examined, and here we focus on three: MIB, the Troxler effect (TE), and perceptual filling-in (PFI). We have selected these three because in all of them a physically present target is repeatedly perceived to alternate between being visible and invisible; in other words, a completely visible stimulus is perceived to simply fade from awareness and then to reappear after some delay. For all three, this subjective experience does not require any special technique, such as a brief target presentation or a flash to induce perceptual transitions, but rather they all occur

spontaneously during natural viewing with maintained fixation. While there are clear differences between each of these phenomena, they all share the commonality that the visually presented stimuli fluctuate in and out of awareness in a seemingly cyclical fashion. Here, we examine these three phenomena within the same participants with the explicit goal of determining if they might be driven by a common underlying mechanism or set of mechanisms.

Motion-induced blindness. In MIB, a static or slowly moving salient target spontaneously disappears for several seconds when superimposed on a moving background (Figure 1(a), Bonneh, Cooperman, & Sagi, 2001). A variety of underlying mechanisms have been suggested for MIB: attentional competition (Bonneh et al., 2001), surface completion (Graf, Adams, & Lages, 2002), interhemispheric rivalry (Carter & Pettigrew, 2003; Funk & Pettigrew, 2003), boundary adaptation (Hsu, Yeh, & Kramer, 2006), perceptual scotoma (New & Scholl, 2008), functional adaptation (Wallis & Arnold, 2009), and a combined effect of adaptation and prolonged inhibition (Gorea & Caetta, 2009). Currently, there is no consensus regarding the mechanisms of MIB, but empirical findings provide evidence for both low- and high-level processes being involved in the illusory disappearances.

The TE. TE (Troxler, 1804), also known as Troxler fading, is the disappearance of a peripherally presented static image which is darker or brighter than its background (Figure 1(b)). A static visible item will perceptually fade such that it disappears into the background. TE has been suggested to manifest from a global mechanism of filling-in that is a basic feature of the human visual system (De Weerd, Smith, & Greenberg, 2006; Komatsu, 2006). Others have suggested that interocular suppression leads to disappearances in TE (Lou, 2008).

Perceptual filling-in. In PFI, a peripheral static patch superimposed on a dynamic noise background disappears and reappears for some period of time (Figure 1(c), Ramachandran & Gregory, 1991). Initially, PFI was designed as an ''artificial scotoma'' and was used as a tool to study spatial and temporal characteristics of the filling-in process that presumably takes place in the blind spot and scotomas (Ramachandran & Gregory, 1991). However, some findings indicate that ''cortical'' adaptation of contours in PFI can contribute to the perceptual fading (Hsieh & Colas, 2012). A boundary adaptation theory points out similarities between MIB and PFI, proposing a shared mechanism for these two phenomena (Hsu, Yeh, & Kramer, 2004; Hsu et al., 2006).

Comparing and Contrasting the Properties of Illusory Disappearances

While each of these phenomena shares important commonalities, little work has systematically studied them in relation to one another. The goal of the current study is to examine possible common mechanisms underlying these phenomena, and there are two broad lines of research that inform this endeavor. First, there is evidence for similar mechanisms for MIB, TE, and PFI that comes from comparing findings across divergent studies. For example, it has been demonstrated that illusory disappearances under MIB (Devyatko, 2011; Geng, Song, Li, Xu, & Zhu, 2007; Schölvinck & Rees, 2009), TE (Lou, 1999), and PFI (De Weerd et al., 2006) can be modulated by attention. In all three phenomena, attended objects (or targets) tend to disappear with higher frequency than unattended objects. Recently, it has also been shown that magnitude of microsaccades decrease before the subjective disappearance of a target and increase right before the

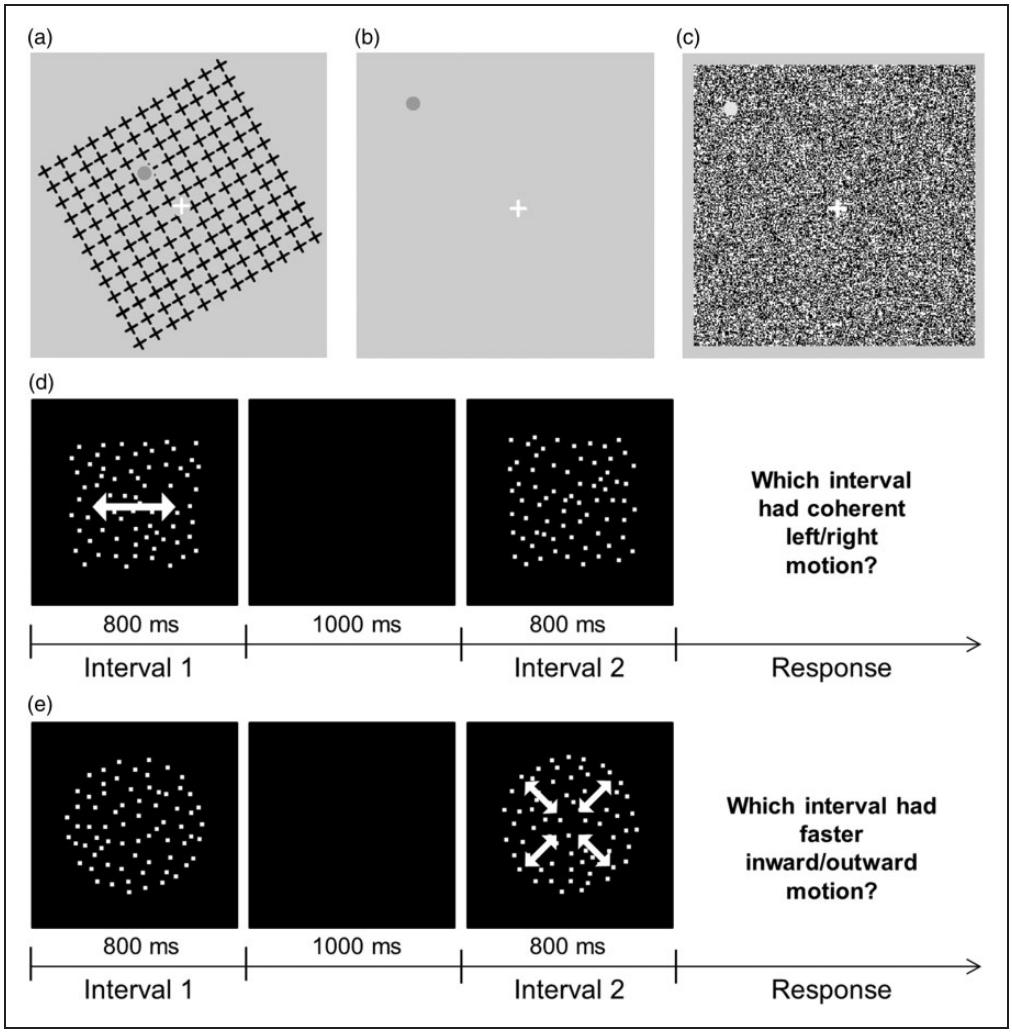

Figure 1. Behavioral stimuli (not to scale—all enlarged for depiction purposes). (a) MIB stimulus. Red fixation cross (shown in white) and a yellow target (shown in gray) on the left were imposed on the rotating blue grid (shown in black). (b) TE stimulus. White fixation cross and a green target (shown in gray) on the left were imposed on a static background. (c) PFI stimulus. Red fixation cross (shown in white) and a gray target on the left were imposed on a dynamic noise background. (d) and (e) Schematic of the stimuli used in the motion coherence detection and motion speed discrimination tasks (white arrows illustrate the direction of dot motion for the two task but were not present in the actual stimuli).

reappearance of a target in MIB (Bonneh et al., 2010; Hsieh & Tse, 2009), TE (Martinez-Conde, Macknik, Troncoso, & Dyar, 2006), and PFI (Troncoso, Macknik, & Martinez-Conde, 2008).

Second, a few studies have explored possible connections between pairs of these phenomena by testing them simultaneously. Based on phenomenological similarity and experimental evidence, a common adaptation mechanism has been suggested for MIB and PFI (Hsu et al., 2006) and for TE and PFI (De Weerd et al., 2006; Komatsu, 2006). For example, it was shown that the duration of disappearances in both MIB and PFI was affected

by the boundary length for occluding targets (Hsu et al., 2006). Likewise, it has been suggested that MIB and TE are both driven, at least in part, by an adaptation mechanism (Bonneh, Donner, Cooperman, Heeger, & Sagi, 2014; Gorea & Caetta, 2009). Particularly, it was shown that all MIB displays with rotating or stationary masks, as well as no masks display, caused a drop in sensitivity for the target, suggesting that adaptation contributed to the illusory disappearances in each condition (Gorea & Caetta, 2009). In addition, another study found that an increase in target contrast significantly reduced mean durations of disappearances for both MIB and TE (Bonneh et al., 2014). However, it should be noted that this study also offered evidence of differences between MIB and TE in that an increase in target contrast doubled the rate of disappearances in MIB and reduced disappearances by half in TE (Bonneh et al., 2014). Collectively, these findings suggest that contrast adaptation contributes to the induction of illusory disappearances in both MIB and TE, but other processes, such as inhibition (Gorea & Caetta, 2009) or neural competition (Bonneh et al., 2014), likely also shape the dynamics of the disappearances in displays like those used in MIB.

It has also been suggested that a common oscillator may underlie similarities in illusory disappearances such that neural activity fluctuates in a similar fashion across different forms of disappearances. For example, binocular rivalry and MIB dominance phase durations were found to be linked such that appearance and disappearance durations in MIB and phases in binocular rivalry could be approximated with a gamma distribution (Carter & Pettigrew, 2003). However, in a recent study comparing temporal dynamics of MIB and binocular rivalry, it was shown that manipulations of target size and luminance contrast had different effects on perceptual fluctuations in these two phenomena (Jaworska & Lages, 2014). Therefore, and in contrast to prior results (Carter & Pettigrew, 2003), it was suggested that MIB and binocular rivalry might not stem from a common oscillator.

When considering the previous research summarized earlier, it is clear that there are arguments for and against a common oscillator account of illusory disappearances in MIB, TE, and PFI. While some studies demonstrated that contrast and eccentricity have similar effects on illusory disappearances in dynamic and static versions of these three phenomena (e.g., Bonneh et al., 2014; Gorea & Caetta, 2009; Hsu et al., 2004), it has also demonstrated that target contrast and target size can have differing effects on the phenomena (e.g., Bonneh et al., 2014; Jaworska & Lages, 2014). The current study will provide further evidence to help clarify this debate.

Given the phenomenological similarities between the MIB, TE, and PFI paradigms, and the suggestive evidence that they are related, it is intriguing to consider the possibility that all three phenomena are driven by a single underlying mechanism. An approach for exploring this common mechanism hypothesis is to compare the temporal dynamics of perceptual alternations among the three phenomena. If they are driven by a common mechanism, there should be meaningful similarities in the temporal dynamics (e.g., the frequency and duration of ''invisible'' states) within an individual. As such, the strategy undertaken here is to assess the temporal characteristics of the visible and invisible states for the three phenomena in a large participant pool to explore possible similarities.

Current Study

In the present study, we tested the possibility that MIB, TE, and PFI stem from a common underlying mechanism. For this purpose, we employed an individual differences approach, wherein we tested the same participants on all three phenomena so that we could explore variability within and across individuals. Although correlational studies are limited in respect

of possible causal interpretation, such an approach is useful when a common latent factor (or a few factors) might potentially explain variability across multiple observed outcome measures. This approach has a long history—with a classic example of trying to reveal a common General Intelligence Factor (Spearman, 1904), and it has recently been used to study the relationship between core cognitive processes (e.g., Huang, Mo, & Li, 2012; Kane, Poole, Tuholski, & Engle, 2006; Sobel, Gerrie, Poole, & Kane, 2007).

Our question here is whether those individuals who experience high rates of MIB disappearances will also tend to experience high rates of illusory disappearances in TE and PFI? That is, are there commonalities in the nature of the participants' experiences that apply across the three phenomena? While this question is relatively simple, adequately answering it can be more difficult. Here, we applied an individual differences approach that rests on the assumption that the quantitative characteristics of disappearances in all three phenomena would correlate with each other if they are driven by a common mechanism. We used a principal component analysis (PCA) approach, which allowed for the extraction of underlying factor(s) without relying on specific *a priori* models or imposing restrictions on statistical distributions of variables (Jolliffe, 2005).

Obtaining meaningful data from an individual differences approach requires variability across participants, and this should not be an issue for the current purposes as previous research has revealed clear variability. First, there are pronounced differences between individuals in their ability to perceive perceptual disappearances in MIB (Carter & Pettigrew, 2003), TE (Lou, 1999), and PFI (Welchman & Harris, 2000). Second, there are systematic differences in the nature of multistable perception between groups of individuals; for example, MIB target disappearances are fewer among individuals with schizophrenia-spectrum disorders compared with a control group (Tschacher, Schuler, & Junghan, 2006). Similarly, individuals with enhanced meditation abilities (e.g., Tibetan Buddhist monks) have demonstrated unusually long durations of illusory disappearances (Carter et al., 2005).

Finally, individuals can vary in a number of other characteristics such as motion sensitivity, overall reaction speed, and their ability to maintain fixation, all of which could potentially be important covariates of illusory disappearances. For example, previous research has shown that increasing mask rotation speed increased disappearances in MIB (Bonneh et al., 2001; Bonneh et al., 2014). Further, the perception of both MIB and PFI has been shown to be altered by the level of motion coherence in the surrounding background (Welchman & Harris, 2000; Wells, Leber, & Sparrow, 2011). Thus, we collected additional data to check whether sensitivity to motion stimuli could explain possible correlations between three phenomena. For this purpose, participants performed separate tasks measuring their thresholds for motion coherence detection and motion speed discrimination. Further, based on findings that reaction time correlates with temporal acuity (Helmbold, Troche, & Rammsayer, 2007), we also measured simple reaction times for our participants. Finally, since previous findings have also shown a link between eye movements and perceptual transitions (Bonneh et al., 2010; Hsieh & Tse, 2009; Martinez-Conde et al., 2006; Troncoso et al., 2008), we tracked eye movements to measure the participants' ability to maintain fixation during the three illusory disappearance tasks.

Methods

Participants

Sixty-nine participants (37 males) completed a single 50-minute testing session that involved multiple assessments. All participants were 18 to 32 years old ($M = 20$), and they were compensated with either $10 or psychology course credit. Participation was voluntarily,

and it was approved by Duke University's Institutional Review Board and conformed to the Code of Ethics of the World Medical Association.

Stimulus and Procedure

Each participant performed five tasks: three illusory disappearance tasks—MIB, TE, and PFI, and two measures of motion sensitivity—a motion coherence detection task and motion speed discrimination task. Eye movements were recorded during the three illusory disappearance tasks. A subset of 29 participants also performed a simple reaction time test. Participants always performed the motion coherence detection, motion speed discrimination, and reaction time tasks first, and then the three illusory disappearance tasks in a randomized order.

Illusory disappearance tasks. Each of the three illusory disappearance tasks started with 30 seconds of practice to make sure the participant understood the procedures and goals. The practice was repeated if the participant needed more exposure or instructions to experience the phenomenon. The practice was followed by the experimental illusory disappearance task that lasted for 240 seconds for each of the three stimulus types. During the experimental phase, the participants were asked to report the instant at which they perceived the attended target to either disappear (via key press on a keyboard) or reappear (releasing the key press), while also maintaining fixation on a central cross. This procedure was used for the MIB, TE, and PFI tasks. Three measures of illusory disappearances were assessed for each participant for each of the illusory disappearance tasks: the number of disappearances, the accumulated (total) duration of disappearances, and the mean episode duration of disappearances (i.e., the mean duration of the disappearances).

Motion-induced blindness. The MIB protocol was adopted from previous research (Mitroff & Scholl, 2004, 2005). The stimulus consisted of a yellow target (RGB color coordinates: R225, G225, B0, $\alpha = 100\%$, size $= 0.58^\circ$), imposed on a rotating grid of blue crosses (RGB color coordinates: R0, G0, B225, $\alpha = 100\%$, size $= 27^\circ \times 27^\circ$, clockwise speed $= 22^\circ/s$), and shown on a black background (see Figure 1(a)). The MIB target was presented 2° above and 2° to the left, of a central red fixation cross.

Troxler effect. The TE stimulus consisted of a green dot (RGB color coordinates: R0, G225, B3, $\alpha = 100\%$, size $= 0.54^\circ$) and presented on a gray background (RGB color coordinates: R204, G204, B204, $\alpha = 100\%$). The target was 4° above and 4° to the left of a white fixation cross (see Figure 1(b)).

Perceptual filling-in. The PFI stimulus consisted of a gray dot (RGB color coordinates: R229, G229, B229, $\alpha = 100\%$, size $= 0.54^\circ$) imposed on a square ($13^\circ \times 13^\circ$) of black and white dynamic noise (see Figure 1(c)). To create dynamic noise, five dissimilar noise images created in Matlab were sequentially presented one by one with each screen refresh. The target was 4° above and 4° to the left of a red fixation cross. The overall background was gray (RGB color coordinates: R204, G204, B204, $\alpha = 100\%$).

Motion sensitivity control tasks. To assess individuals' sensitivity to visual motion, we measured two types of motion thresholds, motion coherence detection and motion speed discrimination. The motion coherence detection and motion speed discrimination tasks were adapted from previous research (Appelbaum, Schroeder, Cain, & Mitroff, 2011) and

were each comprised three blocks. Each block consisted of a response-based staircase procedure to determine the participants' threshold level of sensitivity.

In the motion coherence detection task, participants were asked to identify which of two 800 ms intervals had coherent left or right moving dots, with the other interval containing 0% coherence. In the motion speed discrimination task, participants were asked to discriminate which of two 800 ms intervals had faster radially moving dots, with the slower interval containing a predetermined standard velocity of 6°/s.

In both of these tasks, a two-interval forced-choice staircase procedure was used (Wetherill & Levitt, 1965) that arrived at the minimal discernable stimulus intensity (coherence or velocity). The adaptive staircase followed a correct response by reducing target coherence or speed by 2% (making the next trial harder) and followed an incorrect response with an increase of 4% (making the next trial easier). This one-up or two-down staircase procedure estimates the stimulus level required for each participant to produce 82% correct performance. Individual participant threshold values were computed as the average of three blocks of staircase trials (excluding an initial practice block) for both tasks.

Both motion stimuli consisted of dot fields with 5% dot density and individual dot elements spanning 0.07° of visual angle. The dots were presented in a square field (10° × 10°) for the motion coherence task and circular field (10° diameter) for the speed detection task. On each screen refresh, dots moved 0.17° of visual angle, and 1% of the individual dots were replaced by new, randomly positioned dots. This led to 60% of the dots within a trial being generated a new and 40% remaining for the duration of the trial. The dot contrast was set at 90% of the monitor maximum and appeared as white dots on a black background. The motion coherence detection and motion speed discrimination displays are depicted in Figure 1(d) and (e).

Reaction time control task. A subset of 29 participants also completed a simple reaction time task to assess their speed of response. They completed 75 trials of a target detection task, wherein they were to press the spacebar key as fast as possible after a brief (40 ms) target presentation. The target was a white square (3.35°) presented at the center of the screen against a black background. There was an interstimulus interval of 2 to 5 seconds that was determined by a random, uniform distribution. A white fixation dot in the center of the screen cued the target's location during the interstimulus interval.

Eye-tracking data and analysis. Eye-tracking techniques were employed to continuously measure eye movements throughout the 240-second experimental phase of each of the three illusory disappearances task. The primary purpose of measuring eye movements was to rule out individual differences in the ability to maintain fixation, as previous work has linked eye movement metrics to illusory disappearances (Bonneh et al., 2010; Hsieh & Tse, 2009; Martinez-Conde et al., 2006; Troncoso et al., 2008). The eye tracker used in the current study had a 50 Hz resolution, which did not allow for reliable measures of microsaccades (small eye movements that occur on the millisecond time scale). However, our primary measures of interest were the total number of binocular saccades that exceeded 1° of visual angle and the amplitudes of detected saccades averaged across a trial. Thus, we were able to determine if participants maintained steady fixation on a cross in the center of the screen during any given trial and whether the number of large saccades (indicating poor fixation) negatively correlated with the number of observed disappearances. For correlational analyses, we compared each of these eye movement measures to the illusory disappearances measures. Eye movements were detected by means of an algorithm described in a previous research using eye tracking (Engbert & Kliegl, 2003). Due to technical reasons,

some of the eye-tracking protocols contained signal loss due to a failure to adequately track the eye position. For each illusory disappearance task, eye-tracking data were eliminated from analysis if there was more than 25% signal loss. As a result, we analyzed correlations between behavioral and eye movement data collected from 47 participants for the MIB task, 42 participants for the TE task, and 49 participants for the PFI task.

Apparatus

Computer-based assessments were administered for the MIB, TE, and PFI tasks via a Dell Inspiron computer running Matlab R2010a and the Psychophysics Toolbox-3 (http://psychtoolbox.org). Assessments of motion coherence and motion speed sensitivity were administered on an Apple Macintosh computer running OS9 and the PowerDiva software suite version 3.4. Eye movements were tracked using a Tobii (Deadham, MA) 1750, 50 Hz IR-illuminated video eye tracker. A 17-inch LCD monitor with the default settings from the Tobii eye-tracker setup (75 Hz refresh rate, 1280×1024 resolution) was attached to the Dell computer, and a 19-inch CRT monitor (75 Hz refresh rate, 800×600 resolution) was attached to the Macintosh computer. Participants sat 57 cm from the monitors with their heads supported in a chin rest.

Statistics or Analyses

Principal component analysis. PCA is a well-established approach for reducing the dimensionality of a large dataset to identify structure between variables that might otherwise be hidden. Through PCA, it is possible to identify the underlying components that explain the most variance in a set of measured variables and, therefore, highlight a potentially smaller set of latent constructs that underlie behavior. We used both the Cattell scree test plots and Kaiser criterion (stating that a component should have eigenvalue greater than 1) to determine the number of components. Since only one component passed our selection criteria we did not use rotation.

Comparing temporal dynamics of the phenomena. Some of the previous studies that have investigated a possible common mechanism for multistable phenomena have employed an approximation by gamma distribution (Brascamp, Van Ee, Pestman, & Van Den Berg, 2005; Carter & Pettigrew, 2003). A gamma distribution is a general type of statistical distribution that is commonly used to describe waiting times between Poisson-distributed events; for example, waiting times between phone calls or emails received during a day. Likewise, a previous study has compared the gamma distribution between static and dynamic MIB displays and found both fit well to a gamma function (Gorea & Caetta, 2009). Similar parameters of approximated gamma distributions usually signify a common mechanism often termed a "Poisson clock" (Levelt, 1967). Along with the gamma distribution, lognormal and Weibull distributions have also demonstrated good fits for multistable phenomena such as binocular rivalry, Necker cube, or ambiguous motion (Lehky, 1995; Zhou, Gao, White, Merk, & Yao, 2004). As such, along with gamma distribution, we also assessed the goodness-of-fit for these two distributions to our data.

To compare the temporal dynamics of MIB, TE, and PFI, we took the following steps. First, the duration of disappearances for each task was normalized. To do so, we expressed the duration of each disappearance as a fraction of each participant's mean episode duration. That is, if a participant had a mean episode duration of 0.5 seconds and one of their specific disappearances lasted 0.6 seconds, the specific disappearance was expressed as 0.6/0.5.

This was done for each participant and for the three tasks separately. Second, these normalized data were pooled or aggregated for all observers for each phenomenon separately, and the resulting distributions were compared with each other using a two-sample Kolmogorov-Smirnov test (K-S). Third, we approximated the obtained distributions (normalized durations of MIB, TE, and PFI) to the theoretical distributions of gamma, lognormal, and Weibull using the maximum likelihood estimates and checked a goodness-of-fit with a one-sample Kolmogorov-Smirnov test (K-S). To further test a common mechanism hypothesis, we compared parameters (shape and scale) for the best fitting function (gamma) for all three phenomena.

In addition, we plotted the time series of the mean episode durations and the number of illusory disappearances for MIB, TE, and PFI to compare trends and temporal dynamics of the illusions. For time series analysis, we calculated the number of disappearances, and mean episode duration, for 15-second intervals (i.e., sixteen 15-second intervals over the 240-second trial). Then for every interval, we averaged these numbers and mean episode durations across the 69 participants. These temporal dynamics analyses also allow for the checking of possible adaptation effects in the three phenomena as has been done previously for MIB and TE (Gorea & Caetta, 2009).

Results

The results are presented in three sections later. First, to assess interrelations between the three illusory disappearance tasks, we present descriptive statistics and correlational analyses for illusory disappearances between MIB, TE, and PFI, as well as descriptive statistics and correlational tests for the control measures. Second, we present PCA analyses that specifically test for a possible common mechanism underlying the illusory disappearance phenomena. The illusory disappearances data for correlational tests and PCA are available in open access at Zenodo 10.5281/zenodo.57207. Finally, we present normalized distribution data for the disappearance durations of MIB, TE, and PFI episodes to assess theoretical gamma, lognormal, and Weibull distributions, along with comparisons of their temporal dynamics.

Descriptive Statistics and Correlations

Illusory disappearances. Descriptive statistics for illusory disappearances in MIB, TE, and PFI are presented in Figure 2 and Table 1. There were two participants who had zero disappearances at least in one of the illusions. As depicted in Figure 2, some of the variables contained outliers and extreme values, but for each variable there were no more than four outliers (outliers were defined as data points that were 1.5 times greater than the interquartile range—the magnitude difference between the lower and upper quartile). As well, for each variable, there were no more than three extreme values (defined as data points that were 3 times greater than the interquartile range). We did not remove these observations from the analyses because there were no participants who were outliers for all of the nine variables (and only one participant was an outlier for up to four variables). There were significant correlations between all three illusory disappearance tasks in terms of the total number and the total duration of disappearances[1] (see Figure 3). There were also significant correlations for the mean episode durations between TE and MIB (Kendall's tau = 0.163, $p < .05$) and TE and PFI (Kendall's tau = 0.263, $p < .001$).

Motion sensitivity and reaction times. The results described above reveal a relationship between the three illusory disappearance tasks such that individuals who experience more

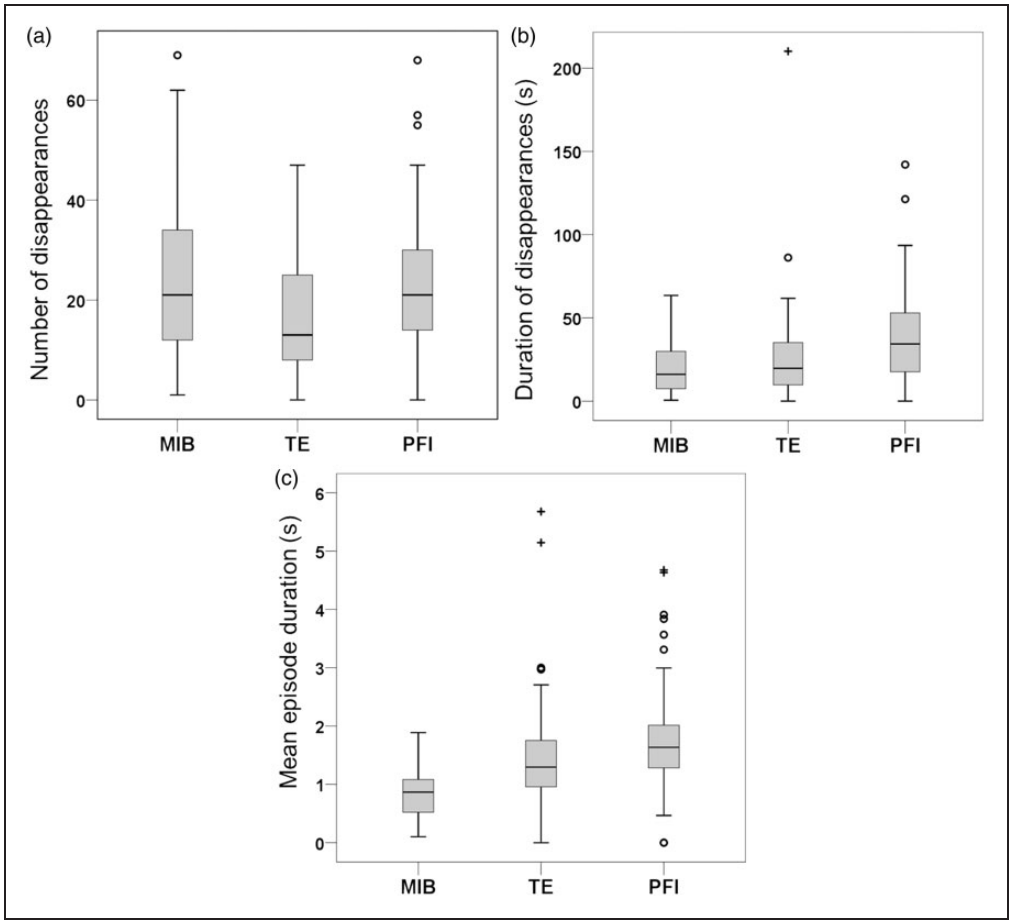

Figure 2. Box-and-whisker plots for disappearances for the motion-induced blindness, Troxler effect, and perceptual filling-in tasks ($N = 69$). (a) Number of disappearances. (b) Total duration of disappearances (seconds). (c) Mean episode duration of disappearances (seconds). For each box-and-whisker plot, the shaded area below the horizontal line indicates the lower quartile, while the shaded area above the line represents the upper quartile. The horizontal line represents the median for that condition, and the whiskers illustrate the minimum and maximum values. The circles represent outliers (>1.5 times the interquartile range) and crosses represent extreme values (>3 times the interquartile range).

MIB = motion-induced blindness; TE = Troxler effect; PFI = perceptual filling-in.

disappearances in one task also experience more disappearances in the other two. This provides an important first step in determining whether a common mechanism underlies all three, but other possible contributing factors need to be considered. All participants completed motion coherence detection and motion speed discrimination tasks to provide assessments of general motion sensitivity (descriptive statistics for these control tasks are in Figure 4). There were no significant correlations between either the motion coherence detection or motion speed discrimination thresholds and any of the measures from the illusory disappearance tasks ($rs < 0.1$, $ps > .05$), suggesting that the observed relationships described earlier are not related to motion sensitivity.

To rule out the participants' reaction time as a contributing factor to the relationships found between the illusory disappearance tasks, we assessed whether reaction times in

Table 1. Descriptive Statistics (*M*, *SD*, Skewness, and Kurtosis) for Total Amount, Total Duration (Seconds), and Mean Episode Duration (Seconds) of Disappearances in MIB, TE, and PFI ($N = 69$).

Phenomena	*M*	*SD*	Skewness	Kurtosis
Motion-induced blindness				
Total number of disappearances	23.70	15.63	.86	.33
Total duration of disappearance	20.01	16.08	.96	.17
Mean episode duration	.84	.40	.49	.04
Troxler effect				
Total number of disappearances	16.32	11.65	.81	−.12
Total duration of disappearance	25.90	29.30	3.91	22.51
Mean episode duration	1.49	.96	2.03	6.70
Perceptual filling-in				
Total number of disappearances	22.23	13.07	1.03	1.80
Total duration of disappearance	39.20	27.26	1.30	2.66
Mean episode duration	1.76	.91	1.21	2.23

a simple detection task correlated with the illusory disappearance task and the motion sensitivity tasks. A one-sample K-S test showed that the distribution of mean reaction times across observers conformed to a normal distribution ($M = 0.29$, $SD = 0.054$). There were no significant correlations between reaction time and any of the illusory disappearances characteristics in any of the three illusory disappearance tasks ($rs < 0.1$, $ps > .05$). The only significant relationship between reaction time and another task was with the motion speed discrimination thresholds (Pearson's $r = 0.4$, $p < .01$), with faster reaction times associated with greater sensitivity to motion speed.

Eye movements. Eye movements were recorded during each of the three illusory disappearance tasks as previous research has found significant relationships between microsaccades and illusory disappearances (Bonneh et al., 2010; Hsieh & Tse, 2009; Martinez-Conde et al., 2006; Troncoso et al., 2008). It is important to demonstrate that the above relationships between the three illusory disappearance tasks were not merely a reflection of how well participants were able to maintain fixation. The mean numbers of "large" saccades were 14.36 ($SD = 13.3$) for MIB, 19.95 ($SD = 18.4$) for TE, and 18.31 ($SD = 16.2$) for PFI. In average, their amplitudes were 63′ ($SD = 34.5'$) in MIB, 75′ ($SD = 29.7'$) in TE, and 77′ ($SD = 28.8'$) in PFI.

No significant correlations were found between the eye movement measures and the disappearance measures for the MIB ($ps > .05$) or TE ($ps > .05$) tasks. These results suggest that eye movements likely do not explain the observed correlations between illusory disappearances.

Principal Component Analysis

Two PCAs were performed across the three illusory disappearance tasks, one for the number of disappearances and one for the accumulated (total) durations of disappearances (for 69 participants). Each PCA analysis revealed a single principal component with an eigenvalue exceeding 1 (2.012 for the number of disappearances, and 1.796 for the total duration of disappearances), with no other components passing the Kaiser criterion. Component loadings for total number of disappearances in MIB, TE, and PFI were 0.83, 0.83, and 0.79, respectively. For total duration of disappearances, loadings were 0.81, 0.73, and 0.78,

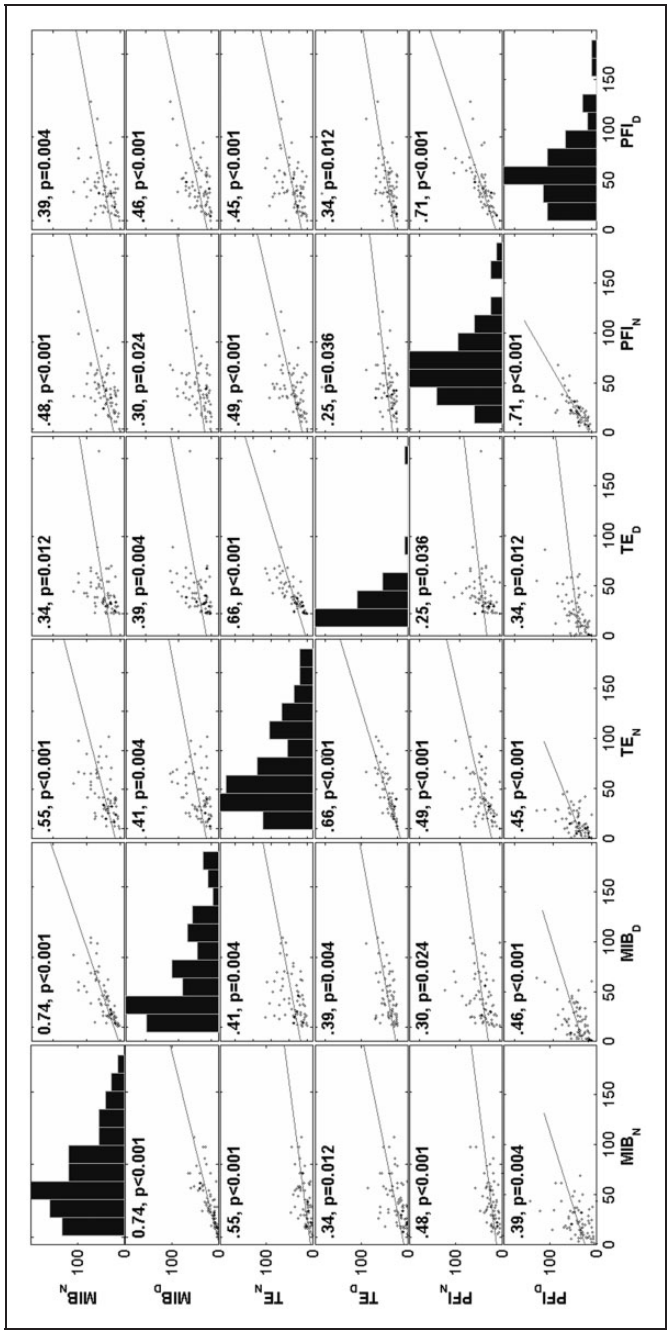

Figure 3. Pearson's correlation coefficients (r) and p values (for $\alpha = 0.05$) adjusted with the Holm-Bonferroni method (Holm, 1979) for total number (N) and total duration (D) of disappearances between MIB, TE, and PFI. [However, before applying Holm-Bonferroni method, four comparisons did not pass the Bonferroni corrected significance level $p = .003$ (unadjusted p values): MIB_N and TE_D, MIB_D and PFI_N, PFI_N and TE_D, PFI_D and TE_D.]
MIB = motion-induced blindness; TE = Troxler effect; PFI = perceptual filling-in.

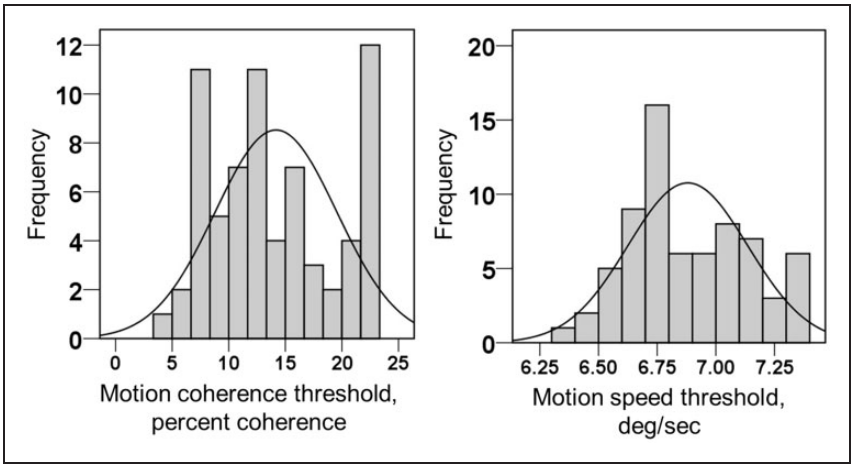

Figure 4. Frequency histograms with normal curve ($N = 69$). Distributions are shown for (a) motion coherence detection ($M = 14.18$, $SD = 5.380$) and (b) motion speed discrimination ($M = 6.88$, $SD = 0.256$) thresholds.

respectively. These single principal components explained 67.0% of the variance for the number of disappearances and 59.8% of the variance for the total durations of illusory disappearances. When combining all data into a single PCA analysis for total numbers and durations of disappearances for all three phenomena, a single principal component was extracted with an eigenvalue of 3.33, which explained 55.5% of variance. Thus, a single principal component explains a large share of the variance across all three stimuli.

Comparing Temporal Dynamics of the Illusory Disappearances

Approximating data with theoretical distributions. As discussed in the section Introduction, an additional way to reveal a potential common mechanism underlying these three illusory disappearance tasks is to compare their temporal dynamics. Following the steps laid out in the section Methods, we first normalized each participant's disappearance duration data by expressing every disappearance as a fraction of the participant's mean episode duration (Carter & Pettigrew, 2003; Levelt, 1967). Importantly, the normalization was done for each of the participants based upon their own data. After the within-participant normalization, we then merged observations from every task into one pool of data for MIB, TE, and PFI correspondingly. That is, we pooled fractions of MIB disappearances across from all participants to create an empirical distribution of MIB, pooled fractions of TE disappearances across participants to create a TE distribution, and pooled the PFI disappearances to create a PFI distribution. The resulting distributions are depicted in Figure 5; each normalized distribution had a mean of 1 with standard deviations of 0.67, 0.70, and 0.71 for MIB, TE, and PFI, respectively. The numbers of disappearances contributing to the normalization varied across tasks: MIB = 1607, TE = 1101, and PFI = 1534.

After normalization, pairwise comparisons of the three tasks were conducted with a two-sample K-S test under the null hypothesis that all three distributions came from a single continuous distribution. Two of the three comparisons fail to reject the null hypothesis (MIB-PFI: K-S $Z = 1.231$, $p = .09$; PFI-TE: K-S $Z = 1.216$, $p = .10$), and one

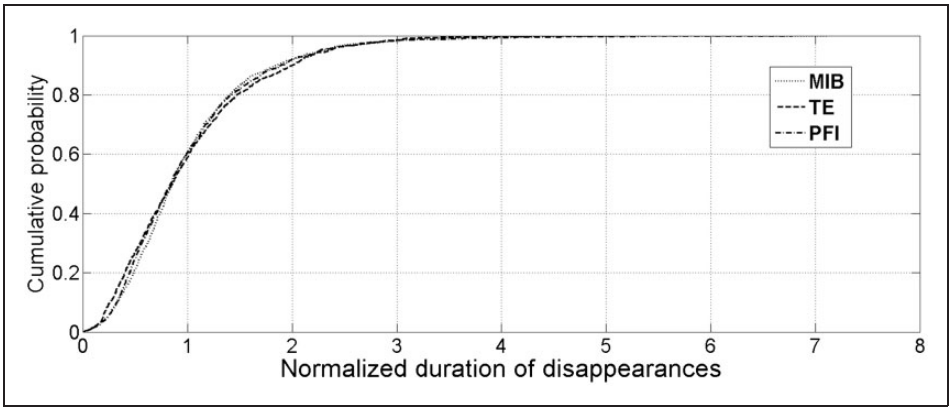

Figure 5. Cumulative distribution functions of illusory disappearances in motion-induced blindness, Troxler effect, and perceptual filling-in ($N = 67$). All disappearance durations are expressed as fractions of the mean duration of disappearances for each participant. Total number of disappearances: MIB = 1607, TE = 1101, PFI = 1534.

MIB = motion-induced blindness; TE = Troxler effect; PFI = perceptual filling-in.

rejects it (MIB-TE: K-S $Z = 1.716$, $p < .01$). These data, therefore, indicate similar temporal dynamics between PFI and the two other phenomena but dissimilar dynamics between MIB and TE.

To examine the extent to which the distributions of illusory disappearances in MIB, TE, and PFI have similar temporal dynamics, we fitted gamma, lognormal, and Weibull distribution models to the data. As depicted in Figures 6 to 8, the best fit for all three tasks was the gamma distribution. All three tasks were not significantly different from the gamma distribution fit (K-S, $ps > .14$), and they were significantly different than the lognormal fit (K-S, $ps < .01$). MIB and PFI were significantly different from the Weibull distribution (K-S, $ps < .01$), but TE was not significantly different from this distribution model (K-S, $p = .36$).

Additional support for a common timing mechanism hypothesis is provided by similar values of parameters approximating a gamma function (shape parameters $a \approx 2$ for all three phenomena). The shape parameter $a = (M/SD)^2$ and the scale parameter $b = (SD)^2/M$, where M and SD are sample mean and standard deviation, respectively. Levelt (1967) suggested that the shape parameter a of the gamma function can reflect the number of ''spikes'' per unit time before an alternation of a competing percept takes place, while the scale parameter b can reflect time interval between two ''spikes.'' In general, these numbers of ''Poison clock'' ticks could vary between individuals but should be consistent for each individual. The Appendix presents illustrative sample data that represent variation between, and consistency within, individuals with ''low,'' ''middle,'' and ''high'' rates of disappearance in MIB, TE, and PFI.

We also fitted gamma distribution models to the raw individual data for the 64 participants (those who had a sufficient number of disappearances in each phenomenon for the distribution fitting procedure) on each task (using maximum likelihood estimates). The mean episode durations of disappearances for these 64 participants were 0.83 (MIB), 1.53 (TE), and 1.83 (PFI). One-sample K-S tests suggested good levels of individual fits ($p > .05$) for MIB (64 participants), TE (64 participants), and PFI (64 participants). However, due to small sample sizes, the test can be less sensitive and these data can reflect a Type II error. The a ($M = 3.8$, $SD = 3.5$ for MIB; $M = 3.9$, $SD = 5.5$ for TE; $M = 2.8$,

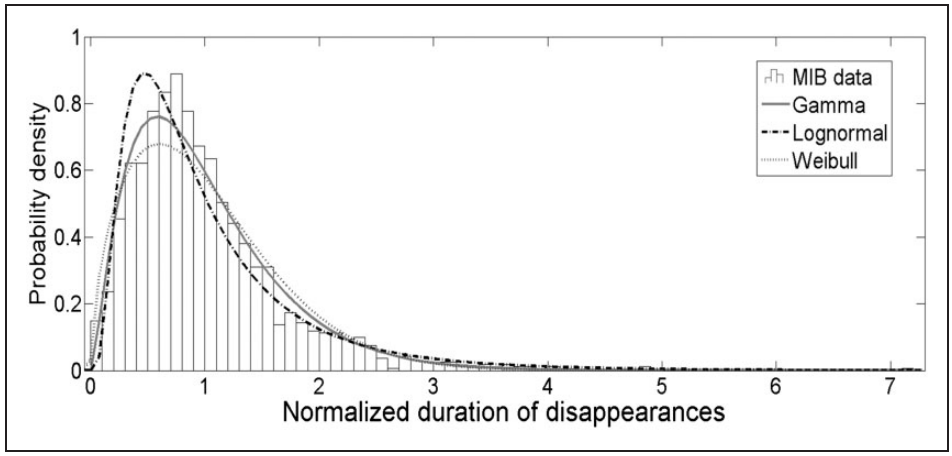

Figure 6. Durations of disappearances under motion-induced blindness (bars) and probability density functions of fitted theoretical models. Parameters of fitted distributions. Gamma: $a = 2.38$ ($SE = 0.08$, 95% CI [2.23, 2.54]), $b = 0.42$ ($SE = 0.02$, 95% CI [0.39, 0.45]), $\mu = 1.00$, $\sigma^2 = 0.42$. Lognormal: mu $= -0.22$ ($SE = 0.02$, 95% CI [−0.26, −0.19]), $\sigma = 0.73$ ($SE = 0.01$, 95% CI [0.71, 0.76]), $\mu = 1.04$, $\sigma^2 = 0.77$. Weibull: $a = 1.12$ ($SE = 0.02$, 95% CI [1.08, 1.15]), $b = 1.59$ ($SE = 0.03$, 95% CI [1.54, 1.65]), $\mu = 1.00$, $\sigma^2 = 0.41$. The data were best explained by the gamma fit and were significantly different from the lognormal and Weibull fits.
MIB = motion-induced blindness.

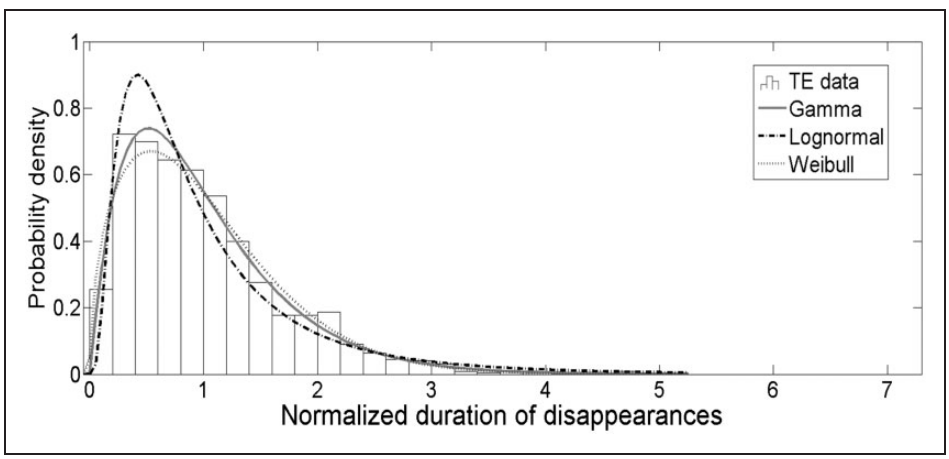

Figure 7. Durations of disappearances under Troxler effect and probability density functions of fitted theoretical models. Parameters of fitted distributions. Gamma: $a = 2.06$ ($SE = 0.08$, 95% CI [1.90, 2.22]), $b = 0.49$ ($SE = 0.02$, 95% CI [0.45, 0.53]), $\mu = 1.00$, $\sigma^2 = 0.49$. Lognormal: mu $= -0.26$ ($SE = 0.02$, 95% CI [− 0.22, −0.31]), $\sigma = 0.78$ ($SE = 0.02$, 95% CI [0.75, 0.82]), $\mu = 1.04$, $\sigma^2 = 0.92$. Weibull: $a = 1.11$ ($SE = 0.02$, 95% CI [1.07, 1.16]), $b = 1.50$ ($SE = 0.03$, 95% CI [1.43, 1.57]), $\mu = 1.00$, $\sigma^2 = 0.46$. The data were best explained by the gamma and Weibull fit and were significantly different from the lognormal fit.
TE = Troxler effect.

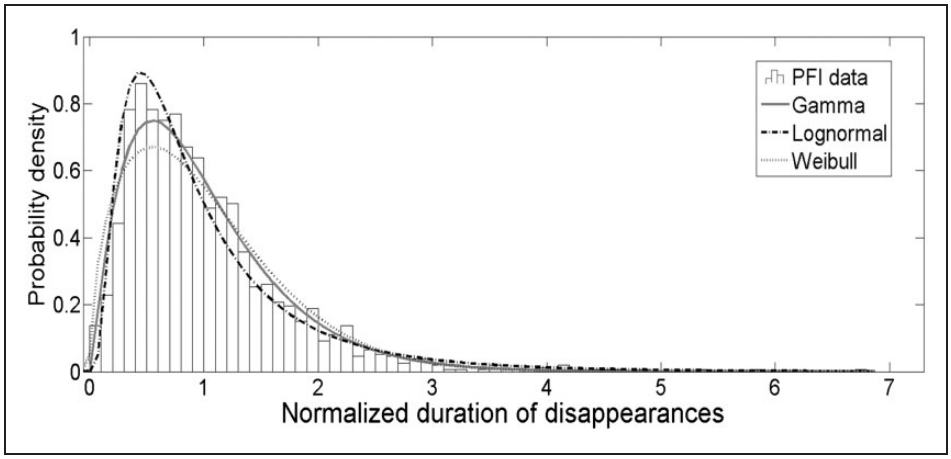

Figure 8. Durations of disappearances under perceptual filling-in and probability density functions of fitted theoretical models. Parameters of fitted distributions. Gamma: $a = 2.22$ ($SE = 0.07$, 95% CI [2.08, 2.37]), $b = 0.45$ ($SE = 0.02$, 95% CI [0.42, 0.48]), $\mu = 1.00$, $\sigma^2 = 0.45$. Lognormal: mu = −0.24 ($SE = 0.02$, 95% CI [−0.20, −0.28]), $\sigma = 0.75$ ($SE = 0.01$, 95% CI [0.73, 0.78]), $\mu = 1.04$, $\sigma^2 = 0.83$. Weibull: $a = 1.11$ ($SE = 0.02$, 95% CI [1.08, 1.15]), $b = 1.52$ ($SE = 0.03$, 95% CI [1.46, 1.57]), $\mu = 1.00$, $\sigma^2 = 0.46$. The data were best explained by the gamma fit and were significantly different from the lognormal and Weibull fits.
PFI = perceptual filling-in.

$SD = 1.5$ for PFI) and b ($M = 0.3$, $SD = 0.3$ for MIB; $M = 0.7$, $SD = 0.7$ for TE; $M = 0.8$, $SD = 0.7$ for PFI) parameters of fitted gamma distributions had large variation between observers. Nevertheless, no significant differences were found for individual values of the parameter compared pairwise between MIB and TE (Wilcoxon's $Z = -1.632$, $p = .103$), MIB and PFI (Wilcoxon's $Z = -1.565$, $p = .118$), or TE and PFI (Wilcoxon's $Z = 0.000$, $p = 1.000$). The b parameter for MIB was significantly different from the b parameters for TE (Wilcoxon's $Z = -4.748$, $p < .001$) and PFI (Wilcoxon's $Z = -6.126$, $p < .001$), but there was no significant difference between the b parameters of TE and PFI individual distributions (Wilcoxon's $Z = -1.190$, $p = .234$).

Time series analysis. Both the number and duration of disappearances are time-dependent measures of illusory disappearances. If a common oscillator (i.e., common timing mechanism) exists, one would expect these measures to show similar dynamics for all three phenomena (cf., Gorea & Caetta, 2009; Wells et al., 2011). To gain a better understanding of timing of illusory disappearances in MIB, TE, and PFI tasks, we calculated how many disappearances happened within each 15-second interval for each phenomenon and plotted the time series for these data over the 240-second stimulus presentation (Figure 9(a)). Similarly, we calculated the mean episode durations in each 15-second interval for each task (Figure 9(b)). Across the three phenomena, the numbers and mean episode durations of disappearances increased during the first 30 seconds of a trial, and then decreased after the first 60 seconds (Figure 9). The increase in the number and mean episode durations of disappearances in the first 30 seconds is consistent with the previous findings (Gorea & Caetta, 2009; Wells et al., 2011) and already established effects of adaptation processes (i.e., higher rate of the phenomena with more exposure). However, the subsequent decrease in the rates following the first 60 seconds of the trial is at odds with adaptation-based mechanisms of disappearances suggesting some other processes taking place.

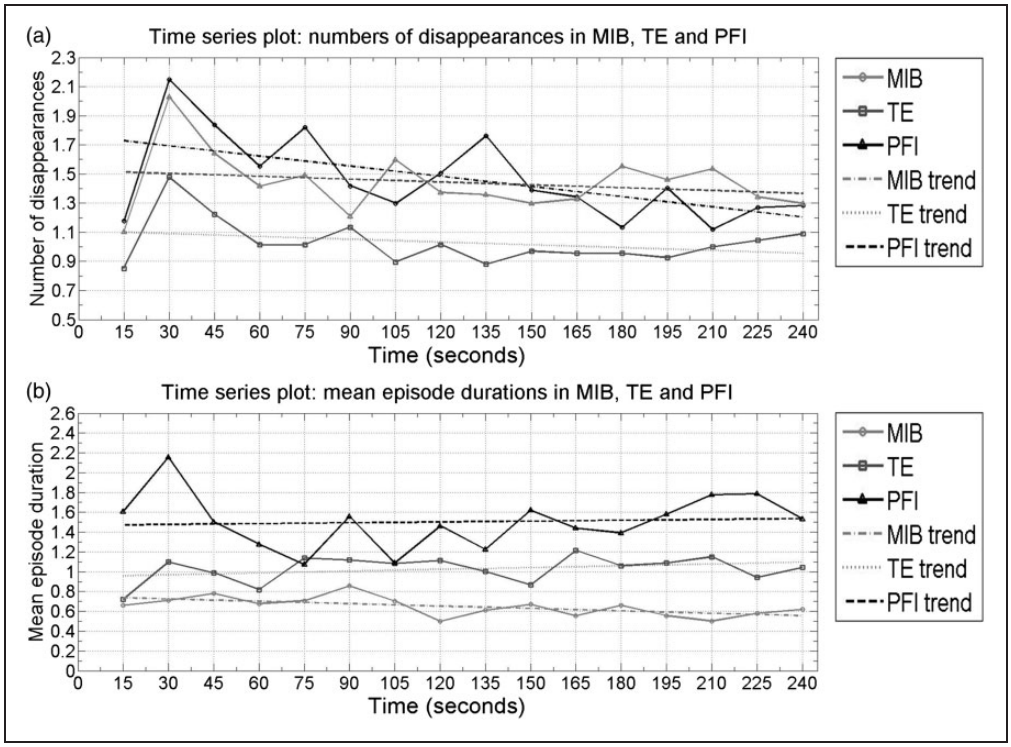

Figure 9. Time series for group data ($N = 67$). Solid lines represent numbers of disappearances (a) and mean episode durations (b) in MIB, TE, and PFI, and dotted lines represent linear trends.
MIB = motion-induced blindness; TE = Troxler effect; PFI = perceptual filling-in.

To further assess possible effects of adaptation on the results, the mean episode durations were compared for participants between the first and fourth minutes of the experimental session for the three illusory disappearances tasks (via paired sample t test). There were no significant differences for MIB (0.8 ± 0.5 vs. 0.7 ± 0.5 seconds; $t = 1.094$, $p = .28$) or PFI (2.01 ± 1.4 vs. 2.01 ± 1.3 seconds; $t = 0.014$, $p = .99$), but there was a significant difference for TE (1.2 ± 0.9 vs. 1.6 ± 1.3 seconds; $t = -2.273$, $p = .03$). These results demonstrate the impact of adaptation processes for TE but not for MIB or PFI. We also calculated slopes for linear trends in TE: for the number of disappearances (Figure 9(a)), the b coefficient was -0.001 ($t = -1.171$, $p = .26$) and for the mean episode duration (Figure 9(b)), the b was 0.001 ($t = 1.301$, $p = .21$), but both linear trend models showed poor fit (adjusted R^2 values of 0.024 and 0.044, respectively). Thus, even if there is an adaptation mechanism contributing to TE, it does not change substantially on the larger time intervals.

Similarly, the numbers of disappearances were compared for participants between the first and fourth minutes of the experimental session for the three illusory disappearances tasks (using paired sample t test). There were no significant differences for TE (4.6 ± 3.8 vs. 4.1 ± 3.5, $t = 1.182$, $p = .24$) or PFI (6.2 ± 3.4 vs. 5.6 ± 3.9, $t = 1.104$, $p = .27$), but there were significantly more disappearances during first minute in MIB (6.7 ± 4.4 vs. 5.1 ± 4.5, $t = 3.193$, $p = .01$). As for the mean episode duration data, these data provide minimal to no support for the cumulative adaptation on large time intervals.

Discussion

Illusory disappearances are an especially interesting class of multistable images as they can occur during natural viewing without any overt manipulation to the stimulus, and thus offer a unique tool for studying visual awareness (Libedinsky & Livingstone, 2011; Panagiotaropoulos et al., 2012). To better understand what underlies the nature of illusory disappearances, the present study explored three specific phenomena: MIB, the TE, and PFI. We used an individual differences approach, wherein commonalities across the three tasks were assessed within and between participants.

The primary hypothesis for the current study was that the three illusory disappearance tasks were driven by a single, common underlying mechanism. We tested this hypothesis by having participants complete the three tasks in one experimental session. Through the use of eye tracking and by administering additional control tasks, we looked to identify other potential covariates of observed correlations between the three phenomena. The results demonstrated moderate to strong correlations between the three tasks, and PCAs revealed that the temporal characteristics of the illusory disappearances could largely be explained by a single component. Further, the eye-tracking metrics and control tasks were not related to the number or duration of illusory disappearances, which suggests that the cross-task correlations and single prinicipal component were not associated with the participants' ability to maintain fixation, their sensitivity to visual motion, or to their overall reaction time. Finally, an analysis of the temporal dynamics for the aggregate data revealed that the normalized durations of disappearances in all three tasks were well fit by a gamma distribution, suggesting that the common mechanism underlying these illusory phenomena may be a timing mechanism, or "oscillator."

It is important to note that given the primary dependent measures in the current study relied on subjective reports, it is difficult to directly determine whether the observed correlations were driven by a common perceptual mechanism or by systematic variation in the participants' decision criterion (i.e., their willingness to report an illusory disappearance). The subjective nature of illusory disappearances, and other phenomena of multistability, is a well-known experimental challenge (e.g., Caetta, Gorea, & Bonneh, 2007; Frässle, Sommer, Jansen, Naber, & Einhäuser, 2014; Mamassian & Goutcher, 2005), and a variety of approaches have been used to offer insight. For example, optokinetic nystagmus and pupil reflex have been used as objective measures of perceptual switches in binocular rivalry (Frässle et al., 2014), showing neural activity associated with perceptual rivalry in the absence of self-report responses. As another approach, participants in one study were asked to report their perceptual interpretation during binocular rivalry only after a beep (Mamassian & Goutcher, 2005). This procedure is in contrast to conventional methods, wherein participants are asked to continuously monitor for perceptual switches. This prompted-reporting procedure minimizes potential ambiguity that can arise between perceptual states and the motor report (i.e., minimizes any potential contamination from the participants' decision criterion). Importantly, the prompted-response procedure provided converging data with previous findings from continuous-report procedures (e.g., producing similar binocular rivalry characteristics such as the gamma distribution of the phase durations; Mamassian & Goutcher, 2005) suggesting that the continuous-report methods are primarily revealing perceptual mechanisms.

In line with the earlier examples, additional previous results also support the assumption that perceptual mechanisms are likely the primary driving forces for the observed correlations found here. First, a recent study was able to dissociate neural correlates of perceptual and decisional processes during multistable perception, suggesting that the decisional processes modulate, but do not cause, perceptual switches (Frässle et al., 2014). Second, it was shown

that gray matter density and cortical thickness in the superior parietal lobe correlated with individuals' alternation rate for a bistable structure-from-motion stimulus (Kanai, Bahrami, & Rees, 2010). This is supportive of a perceptual account of alternations given that the superior parietal lobule is thought to underlie the perceptual dynamics in multistable perception (Carmel, Walsh, Lavie, & Rees, 2010; Kanai, Carmel, Bahrami, & Rees, 2011; Zaretskaya, Thielscher, Logothetis, & Bartels, 2010). Furthermore, in the same study, transcranial magnetic stimulation of bilateral superior parietal lobule regions led to a decrease in the alternation rate, suggesting a causal role of these regions in bistable perception of structure-from-motion stimulus (Kanai et al., 2010). Third, a twins study of binocular rivalry found higher correlations of alternation rates between monozygotic twins in comparison to dizygotic twins, and the best fitting model accounted for more than half of the variance in binocular rivalry rate by additive genetic factors (Miller et al., 2010). Finally, it is also noteworthy that several functional magnetic resonance imaging and electroencephalogram illusory disappearances studies have used a yoked-replay method, wherein a stimulus is physically removed from a display according to the time stamps collected from the participants' subjective reports (i.e., they replay the participants their own disappearance experience with physical, rather than illusory, disappearances). The comparisons of neural activity during the subjective disappearances and the physical removal of targets revealed some differences, but mostly in brain areas related to visual perception (e.g, Donner, Sagi, Bonneh, & Heeger, 2008; Matsuzaki et al., 2012; Mendola, Conner, Sharma, Bahekar, & Lemieux, 2006; Schölvinck & Rees, 2010).

Recent research has tested whether response bias (i.e., the tendency of a participant to misreport illusory disappearances or alternations in other forms of perceptual rivalry) is correlated with observed illusory alternations (Gallagher & Arnold, 2014). This research found a correlation between reported alternations in binocular rivalry and reported changes of a physical stimulus mimicking binocular rivalry reversals, however, this relation was found only in one out of three experiments with binocular rivalry. Importantly, there were no such correlations between reported changes in the mimicking stimulus and reported disappearances in MIB or alternations in Necker cube (Gallagher & Arnold, 2014). Although it is questionable whether the same criterion is used for the physical and the subjective (illusory) changes and whether the same criterion is used for each type of illusions, we find this preliminary result very inspiring. Controlling for misreports in future studies of multistable perception is important for clarifying this issue.

In sum, more work is needed to definitively state that the observed correlations found here are driven by perceptual mechanisms, but the existing literature mostly supports such a conclusion, though the possible contribution from decisional factors cannot be easily discarded.

Taken together, these results suggest that the observed commonalities may stem from a shared temporal component. That said, while the current evidence points toward a shared mechanism account of perceptual disappearances across these forms of illusory disappearances, this inference follows from correlational relationships. Future experimental manipulations could be implemented to offer causal support. Later, we discuss the current findings in light of previous studies and highlight the strengths and weaknesses in inferences that can be gained from these results.

The findings reported here suggest that correlations between MIB, TE, and PFI can be largely explained by a common timing mechanism in a form of an ''oscillator''—a stochastic process(es) in the visual system that sets temporal characteristics of perceptual alternations for phenomena of illusory disappearances and, possibly, for other multistable phenomena. This concept of a common oscillator has previously been proposed in a correlational study as

an underlying mechanism for both binocular rivalry and MIB (Carter & Pettigrew, 2003), as a shared timing mechanism that explains intraindividual similarity between the two phenomena, despite variation among individuals in the ability to perceive illusory reversals. Although descriptive statistics of the raw data indicate some difference between distributions of the three phenomena, the current data are consistent with this hypothesis as the total number and total duration of disappearances were both found to be strongly correlated across the three tasks of MIB, TE, and PFI. Moreover, the distributions of normalized mean episode durations of disappearances in MIB, TE, and PFI were all well fit by a gamma distribution suggesting a common underlying mechanism for these phenomena. Contrasting pairs of the distributions demonstrated that disappearances under MIB and PFI, as well as under PFI and TE could be evoked by the same oscillatory process. As such, this oscillatory process, or ''Poisson clock'' (Levelt, 1967), can be responsible for the similar patterns of disappearances during MIB, TE, and PFI.

Such oscillator mechanisms have been experimentally linked to neuronal spike timing properties of the visual system for a number of different perceptual processes (e.g., Jensen et al., 2012; Wilson, Blake, & Lee, 2001). For example, the spatial propagation of perceptual dominance in binocular rivalry has been characterized by temporally precise, traveling waves of cortical activity that are governed by similar clock mechanisms (Lee, Blake, & Heeger, 2005). An alternative explanation of the obtained between-individual differences and within-individual consistency in temporal dynamics comes from another correlational study, which demonstrated that individuals with higher levels of inhibitory neurotransmitter gamma-aminobutyric acid tended to have longer durations of perceptual states in MIB, binocular rivalry, and structure-from-motion (van Loon et al., 2013). However, there is evidence that multiple low and high cortical areas change their activity in correspondence with perceptual alternations (Donner et al., 2008; Hsieh & Tse, 2009; Mendola et al., 2006; Schölvinck & Rees, 2010). Recently, it was shown for MIB that fluctuations of activity in target-specific subregions of V1 and V4 correlated with the duration and rate of disappearances, correspondingly (Donner, Sagi, Bonneh, & Heeger, 2013). As such, it is possible that the single principal component revealed here for the total duration and number of disappearances might reflect information processing in these subregions or interactions between these processes. In turn, a similar pattern of microsaccades around a perceptual reversal in MIB, TE, and PFI (Bonneh et al., 2010; Hsieh & Tse, 2009; Martinez-Conde et al., 2006; Troncoso et al., 2008) suggests that the observed common temporal dynamics of these three illusions can possibly stem from a mechanism producing a perimicrosaccadic alternations in perceptions (Hafed, 2013). In addition, recent studies demonstrated a link between miscrosaccades and shifts in visual attention (Hafed, 2013; Hafed, Goffart, & Krauzlis, 2009; Yuval-Greenberg, Merriam, & Heeger, 2014). Whereas attention modulates illusory disappearances in MIB, TE, and PFI in the same fashion (Devyatko, 2011; De Weerd et al., 2006; Geng et al., 2007; Lou, 1999; Schölvinck & Rees, 2009), the mechanism producing similar patterns of microsaccades in the three illusions can be also modulated by shifts in attention.

It is also worth considering the role of adaptation in the observed commonalities between MIB, TE, and PFI. Previous research has suggested that an adaptation process (e.g., De Weerd, Desimone, & Ungerleider, 1998) could determine illusory disappearances in MIB and PFI (Hsu et al., 2004, 2006) as well as in TE and PFI (De Weerd et al., 2006). One possible influence of adaptation across these phenomena is an increasing duration or rate of disappearances over the course of a trial (Gorea & Caetta, 2009; Wells et al., 2011); however, we found minimal evidence for such an effect here. That said, the previous studies used shorter trial lengths ($\leq$60 seconds) than what was used here (240 seconds).

When assessing just the first 20 to 60 seconds of the current data (Figure 9(a) and (b)), the mean episode durations and numbers of illusory disappearances in MIB, TE, and PFI were in agreement with previous findings (Gorea & Caetta, 2009; Wells et al., 2011). As such, it appears that with longer trial lengths adaptation reaches plateau (Gorea & Caetta, 2009; Wells et al., 2011) as revealed by the temporal dynamics of illusory disappearances. In line with the other indirect evidence, we did not find significant correlations between times before first disappearances for the three phenomena. However, future experiments can help to clarify the role of adaptation in these three phenomena.

According to an adaptation account the longer durations of disappearances would be observed during the fourth minute of a trial as compared with the first minute due to enhanced adaptation. For MIB and PFI, there were no significant differences in mean episode duration between first and fourth minutes, indicating that it is unlikely that such adaptation took place. However, for TE, this difference was significant. This dissimilarity between TE and two other phenomena might be partly explained by the fact that MIB and PFI employed dynamic displays, whereas the TE stimulus was static. This result is in line with a recent study showing that altering target contrast had opposite effects on dynamic and static displays; when contrast was increased, the number of disappearances increased in MIB and decreased in TE (Bonneh et al., 2014). Previous research suggests that dynamic backgrounds can lead to competition or mutual suppression between backgrounds and targets that caused a shift in the purported adaptation process (Bonneh et al., 2014; Gorea & Caetta, 2009; Libedinsky, Savage, & Livingstone, 2009). Alternative possible explanation comes from a recent study of contrast sensitivity changes during dominance and suppression phases in binocular rivalry (Alais, Cass, O'Shea, & Blake, 2010). This research revealed that only for the half of participants contrast thresholds decreased during suppression episodes in binocular rivalry assuming that adaptation yielding episodes of suppression can vary between individuals (Alais et al., 2010). If similar individual differences in contrast sensitivity changes take place during disappearances in MIB and PFI, this could explain why we did not find accumulation of adaptation during the trial on the group level.

It is important to note that while we found moderate to strong correlations between MIB, TE, and PFI, another recent study failed to find significant interrelations for another set of multistable phenomena, namely, between MIB, binocular rivalry, and Necker cube (Gallagher & Arnold, 2014). We did not include binocular rivalry and Necker cube in the current study for several reasons. First, these illusions phenomenologically are slightly different from the illusory disappearances phenomena. One can easily find the difference between perceiving illusory disappearances (e.g., in TE) and alternations between two interpretations of the same stimuli (Necker cube), or alternations between two dichoptically presented images (binocular rivalry). Second, in contrast to Gallaher and Arnold (2014), we did not aim to replicate the previous studies, comparing MIB and binocular rivalry (Carter & Pettigrew, 2003, see also Jaworska & Lages, 2014). While we used other phenomena (except MIB), it is still useful to make our studies comparable. Therefore, we calculated alternation rates for MIB, TE, and PFI: the mean alternations rates for MIB, TE, and PFI are 0.0987($SD = 0.065$), 0.0680 ($SD = 0.049$), and 0.0926 ($SD = 0.054$), respectively. We found significant correlations between all pairs of alternation rates ($ps < .001$ for all comparisons): Pearson's r were 0.480 (for MIB and PFI), 0.552 (for MIB and TE), and 0.485 (for TE and PFI). Therefore, we observed the significant interrelations between these three illusions. However, the meta-analysis of aggregated data from ours and other relevant studies should help in clarifying the issue of inconsistency of results concerning temporal dynamics of different multistable phenomena.

In summary, the data reported here, in conjunction with previous findings, suggest that illusory disappearances are primarily driven by a common timing mechanism in the form of an oscillator. The oscillator mechanism likely reflects nonspecific, general properties of the visual system that underlie multiple processes (e.g., van Loon et al., 2013; Wilson et al., 2001). The current study is the first to empirically demonstrate that MIB, TE, and PFI are all driven by this general timing mechanism. Moreover, whereas previous studies exploring commonalities between MIB, TE, and PFI have done so by making the tasks more similar to one another to control for potential contaminating sensory factors (e.g., Bonneh et al., 2014; Gorea & Caetta, 2009; Hsu et al., 2004, 2006), the current study has taken an individual differences approach that does not substantially modify the stimuli. This leaves intact the basic constructs that are typically used to induce these types of illusory disappearances, making the current comparisons perhaps more directed as they use each phenomena's typical methods. As such, we feel this approach offers an exciting direction to take for further studies addressing the behavioral and brain processes underlying the perception of multistable images.

Acknowledgements

This project was completed in the Duke Visual Cognition Lab. At the time of data collection, D. Devyatko and S. Mitroff were affiliated with Duke University's Department of Psychology and Neuroscience and Center for Cognitive Neuroscience. The authors thank Matthew Cain, Joe Harris, Elise Darling, Lydia Ran, and the Duke Visual Cognitive Lab for their help.

Declaration of Conflicting Interests

The author(s) declared no potential conflicts of interest with respect to the research, authorship, and/or publication of this article.

Funding

The author(s) disclosed receipt of the following financial support for the research, authorship, and/or publication of this article: This work was partially supported by a Fulbright Scholarship awarded to D. Devyatko and Army Research Office Grant #W911NF-09-1-0092 awarded to S. Mitroff.

Note

1. We also analyzed the time of the first disappearance in each trial (data not shown). No significant correlations between MIB, TE, and PFI were found for the time of first disappearances. TE started significantly later than MIB ($p = .02$) and near significantly later than PFI ($p = .055$). There was no significant difference between time of the first disappearances between MIB and PFI. Mean times of the first disappearances were 17.69 ($SD = 24.47$) for MIB, 24.33 ($SD = 33.72$) for TE, and 14.32 ($SD = 14.75$) for PFI.

References

Alais, D., Cass, J., O'Shea, R. P., & Blake, R. (2010). Visual sensitivity underlying changes in visual consciousness. *Current Biology: CB*, *20*, 1362–1367. doi:10.1016/j.cub.2010.06.015

Appelbaum, L. G., Schroeder, J. E., Cain, M. S., & Mitroff, S. R. (2011). Improved visual cognition through stroboscopic training. *Frontiers in Psychology*, *2*, 276. doi:10.3389/fpsyg.2011.00276

Blake, R. (2001). A primer on binocular rivalry, including current controversies. *Brain and Mind*, *2*, 5–38. doi:10.1023/A:1017925416289

Bonneh, Y., Cooperman, A., & Sagi, D. (2001). Motion-induced blindness in normal observers. *Nature*, *411*, 798–801. doi:10.1038/35081073

Bonneh, Y., Donner, T. H., Sagi, D., Fried, M., Cooperman, A., Heeger, D. J., . . . Arieli, A. (2010). Motion-induced blindness and microsaccades: Cause and effect. *Journal of Vision*, *10*, 22. doi:10.1167/10.14.22

Bonneh, Y. S., Donner, T. H., Cooperman, A., Heeger, D. J., & Sagi, D. (2014). Motion-induced blindness and Troxler fading: Common and different mechanisms. *PloS One*, *9*, e92894. doi:10.1371/journal.pone.0092894

Brascamp, J. W., Van Ee, R., Pestman, W. R., & Van Den Berg, A. V. (2005). Distributions of alternation rates in various forms of bistable perception. *Journal of Vision*, *5*, 287–298. doi:10:1167/5.4.1

Brugger, P., & Brugger, S. (1993). The Easter bunny in October: Is it disguised as a duck? *Perceptual and Motor Skills*, *76*, 557–558.

Caetta, F., Gorea, A., & Bonneh, Y. (2007). Sensory and decisional factors in motion-induced blindness. *Journal of Vision*, *7*, 4.1–12. doi:10.1167/7.7.4

Carmel, D., Walsh, V., Lavie, N., & Rees, G. (2010). Right parietal TMS shortens dominance durations in binocular rivalry. *Current Biology: CB*, *20*, R799–R800. doi:10.1016/j.cub.2010.07.036

Carter, O. L., & Pettigrew, J. D. (2003). A common oscillator for perceptual rivalries? *Perception*, *32*, 295–305.

Carter, O. L., Presti, D. E., Callistemon, C., Ungerer, Y., Liu, G. B., & Pettigrew, J. D. (2005). Meditation alters perceptual rivalry in Tibetan Buddhist monks. *Current Biology: CB*, *15*, R412–R413. doi:10.1016/j.cub.2005.05.043

Chong, S. C., & Blake, R. (2006). Exogenous attention and endogenous attention influence initial dominance in binocular rivalry. *Vision Research*, *46*, 1794–1803. doi:10.1016/j.visres.2005.10.031

Devyatko, D. (2011). Attentional distribution affects motion-induced blindness. *Journal of Russian and East European Psychology*, *49*, 30–44. doi:10.2753/RPO1061-0405490502

De Weerd, P., Desimone, R., & Ungerleider, L. G. (1998). Perceptual filling-in: A parametric study. *Vision Research*, *38*, 2721–2734.

De Weerd, P., Smith, E., & Greenberg, P. (2006). Effects of selective attention on perceptual filling-in. *Journal of Cognitive Neuroscience*, *18*, 335–347. doi:10.1162/089892906775990561

Donner, T. H., Sagi, D., Bonneh, Y. S., & Heeger, D. J. (2008). Opposite neural signatures of motion-induced blindness in human dorsal and ventral visual cortex. *The Journal of Neuroscience: The Official Journal of the Society for Neuroscience*, *28*, 10298–10310. doi:10.1523/JNEUROSCI.2371-08.2008

Donner, T. H., Sagi, D., Bonneh, Y. S., & Heeger, D. J. (2013). Retinotopic patterns of correlated fluctuations in visual cortex reflect the dynamics of spontaneous perceptual suppression. *The Journal of Neuroscience: The Official Journal of the Society for Neuroscience*, *33*, 2188–2198. doi:10.1523/JNEUROSCI.3388-12.2013

Engbert, R., & Kliegl, R. (2003). Microsaccades uncover the orientation of covert attention. *Vision Research*, *43*, 1035–1045.

Frässle, S., Sommer, J., Jansen, A., Naber, M., & Einhäuser, W. (2014). Binocular rivalry: Frontal activity relates to introspection and action but not to perception. *The Journal of Neuroscience: The Official Journal of the Society for Neuroscience*, *34*, 1738–1747. doi:10.1523/JNEUROSCI.4403-13.2014

Funk, A. P., & Pettigrew, J. D. (2003). Does interhemispheric competition mediate motion-induced blindness? A transcranial magnetic stimulation study. *Perception*, *32*, 1325–1338.

Gallagher, R. M., & Arnold, D. H. (2014). Interpreting the temporal dynamics of perceptual rivalries. *Perception*, *43*, 1239–1248.

Geng, H., Song, Q., Li, Y., Xu, S., & Zhu, Y. (2007). Attentional modulation of motion-induced blindness. *Chinese Science Bulletin*, *52*, 1063–1070. doi:10.1007/s11434-007-0178-0

Gorea, A., & Caetta, F. (2009). Adaptation and prolonged inhibition as a main cause of motion-induced blindness. *Journal of Vision*, *9*, 16.1–17. doi:10.1167/9.6.16

Graf, E. W., Adams, W. J., & Lages, M. (2002). Modulating motion-induced blindness with depth ordering and surface completion. *Vision Research*, *42*, 2731–2735.

Hafed, Z. M. (2013). Alteration of visual perception prior to microsaccades. *Neuron*, *77*, 775–786. doi:10.1016/j.neuron.2012.12.014

Hafed, Z. M., Goffart, L., & Krauzlis, R. J. (2009). A neural mechanism for microsaccade generation in the primate superior colliculus. *Science*, *323*, 940–943. doi:10.1126/science.1166112

Helmbold, N., Troche, S., & Rammsayer, T. (2007). Processing of temporal and nontemporal information as predictors of psychometric intelligence: A structural-equation-modeling approach. *Journal of Personality*, *75*, 985–1006. doi:10.1111/j.1467-6494.2007.00463.x

Hsieh, P.-J., & Colas, J. T. (2012). Perceptual fading without retinal adaptation. *Journal of Experimental Psychology. Human Perception and Performance*, *38*, 267–271. doi:10.1037/a0026963

Hsieh, P.-J., & Tse, P. U. (2009). Microsaccade rate varies with subjective visibility during motion-induced blindness. *PloS One*, *4*, e5163. doi:10.1371/journal.pone.0005163

Hsu, L.-C., Yeh, S.-L., & Kramer, P. (2004). Linking motion-induced blindness to perceptual filling-in. *Vision Research*, *44*, 2857–2866. doi:10.1016/j.visres.2003.10.029

Hsu, L.-C., Yeh, S.-L., & Kramer, P. (2006). A common mechanism for perceptual filling-in and motion-induced blindness. *Vision Research*, *46*, 1973–1981. doi:10.1016/j.visres.2005.11.004

Huang, L., Mo, L., & Li, Y. (2012). Measuring the interrelations among multiple paradigms of visual attention: An individual differences approach. *Journal of Experimental Psychology. Human Perception and Performance*, *38*, 414–428. doi:10.1037/a0026314

Jastrow, J. (1899). The mind's eye. *Popular Science Monthly*, *54*, 299–312.

Jaworska, K., & Lages, M. (2014). Fluctuations of visual awareness: Combining motion-induced blindness with binocular rivalry. *Journal of Vision*, *14*, 11. doi:10.1167/14.11.11

Jensen, O., Bonnefond, M., & VanRullen, R. (2012). An oscillatory mechanism for prioritizing salient unattended stimuli. *Trends in Cognitive Sciences*, *16*, 200–206. doi:10.1016/j.tics.2012.03.002

Jolliffe, I. (2005). Principal component analysis. In Brian S. E., & David C. H. (Eds.), *Encyclopedia of Statistics in Behavioral Science* (Vol. 3, Chichester, pp.1580–1584). Hoboken, NJ: John Wiley and Sons, Ltd.

Kanai, R., Bahrami, B., & Rees, G. (2010). Human parietal cortex structure predicts individual differences in perceptual rivalry. *Current Biology: CB*, *20*, 1626–1630. doi:10.1016/j.cub.2010.07.027

Kanai, R., Carmel, D., Bahrami, B., & Rees, G. (2011). Structural and functional fractionation of right superior parietal cortex in bistable perception. *Current Biology: CB*, *21*, R106–R107. doi:10.1016/j.cub.2010.12.009

Kane, M. J., Poole, B. J., Tuholski, S. W., & Engle, R. W. (2006). Working memory capacity and the top-down control of visual search: Exploring the boundaries of "executive attention." *Journal of Experimental Psychology. Learning, Memory, and Cognition*, *32*, 749–777. doi:10.1037/0278-7393.32.4.749

Kim, C., & Blake, R. (2005). Psychophysical magic: Rendering the visible "invisible.". *Trends in Cognitive Sciences*, *9*, 381–388. doi:10.1016/j.tics.2005.06.012

Komatsu, H. (2006). The neural mechanisms of perceptual filling-in. *Nature Reviews Neuroscience*, *7*, 220–231. doi:10.1038/nrn1869

Lee, S.-H., Blake, R., & Heeger, D. J. (2005). Traveling waves of activity in primary visual cortex during binocular rivalry. *Nature Neuroscience*, *8*, 22–23. doi:10.1038/nn1365

Lehky, S. R. (1995). Binocular rivalry is not chaotic. *Proceedings. Biological Sciences/The Royal Society*, *259*, 71–76. doi:10.1098/rspb.1995.0011

Leopold, D. A., & Logothetis, N. K. (1999). Multistable phenomena: Changing views in perception. *Trends in Cognitive Sciences*, *3*, 254–264. doi:10.1016/S1364-6613(99)01332-7

Levelt, W. J. (1967). Note on the distribution of dominance times in binocular rivalry. *British Journal of Psychology (London, England: 1953)*, *58*, 143–145.

Libedinsky, C., & Livingstone, M. (2011). Role of prefrontal cortex in conscious visual perception. *The Journal of Neuroscience: The Official Journal of the Society for Neuroscience*, *31*, 64–69. doi:10.1523/JNEUROSCI.3620-10.2011

Libedinsky, C., Savage, T., & Livingstone, M. (2009). Perceptual and physiological evidence for a role for early visual areas in motion-induced blindness. *Journal of Vision*, *9*, 14.1–10. doi:10.1167/9.1.14

Lou, L. (1999). Selective peripheral fading: Evidence for inhibitory sensory effect of attention. *Perception*, *28*, 519–526.

Lou, L. (2008). Troxler effect with dichoptic stimulus presentations: Evidence for binocular inhibitory summation and interocular suppression. *Vision Research*, *48*, 1514–1521. doi:10.1016/j.visres.2008.04.001

Mamassian, P., & Goutcher, R. (2005). Temporal dynamics in bistable perception. *Journal of Vision*, *5*, 361–375. doi:10:1167/5.4.7

Martinez-Conde, S., Macknik, S. L., Troncoso, X. G., & Dyar, T. A. (2006). Microsaccades counteract visual fading during fixation. *Neuron*, *49*, 297–305. doi:10.1016/j.neuron.2005.11.033

Matsuzaki, N., Juhász, C., & Asano, E. (2012). Oscillatory modulations in human fusiform cortex during motion-induced blindness: Intracranial recording. *Clinical Neurophysiology: Official Journal of the International Federation of Clinical Neurophysiology*, *123*, 1925–1930. doi:10.1016/j.clinph.2012.02.085

Mendola, J. D., Conner, I. P., Sharma, S., Bahekar, A., & Lemieux, S. (2006). fMRI measures of perceptual filling-in in the human visual cortex. *Journal of Cognitive Neuroscience*, *18*, 363–375. doi:10.1162/089892906775990624

Meng, M., & Tong, F. (2004). Can attention selectively bias bistable perception? Differences between binocular rivalry and ambiguous figures. *Journal of Vision*, *4*, 539–551. doi:10:1167/4.7.2

Miller, S. M., Hansell, N. K., Ngo, T. T., Liu, G. B., Pettigrew, J. D., Martin, N. G., . . . Wright, M. J. (2010). Genetic contribution to individual variation in binocular rivalry rate. *Proceedings of the National Academy of Sciences of the United States of America*, *107*, 2664–2668. doi:10.1073/pnas.0912149107

Mitroff, S., & Scholl, B. (2005). Forming and updating object representations without awareness: Evidence from motion-induced blindness. *Vision Research*, *45*, 961–967.

Mitroff, S. R., & Scholl, B. J. (2004). Seeing the disappearance of unseen objects. *Perception*, *33*, 1267–1273.

New, J. J., & Scholl, B. J. (2008). ''Perceptual scotomas'': A functional account of motion-induced blindness. *Psychological Science*, *19*, 653–659. doi:10.1111/j.1467-9280.2008.02139.x

Panagiotaropoulos, T. I., Deco, G., Kapoor, V., & Logothetis, N. K. (2012). Neuronal discharges and gamma oscillations explicitly reflect visual consciousness in the lateral prefrontal cortex. *Neuron*, *74*, 924–935. doi:10.1016/j.neuron.2012.04.013

Panagiotaropoulos, T. I., Kapoor, V., Logothetis, N. K., & Deco, G. (2013). A common neurodynamical mechanism could mediate externally induced and intrinsically generated transitions in visual awareness. *PloS One*, *8*, e53833. doi:10.1371/journal.pone.0053833

Parkkonen, L., Andersson, J., Hämäläinen, M., & Hari, R. (2008). Early visual brain areas reflect the percept of an ambiguous scene. *Proceedings of the National Academy of Sciences of the United States of America*, *105*, 20500–20504. doi:10.1073/pnas.0810966105

Pitts, M. A., Martínez, A., Stalmaster, C., Nerger, J. L., & Hillyard, S. A. (2009). Neural generators of ERPs linked with Necker cube reversals. *Psychophysiology*, *46*, 694–702. doi:10.1111/j.1469-8986.2009.00822.x

Pitts, M. A., Nerger, J. L., & Davis, T. J. R. (2007). Electrophysiological correlates of perceptual reversals for three different types of multistable images. *Journal of Vision*, *7*, 6. doi:10.1167/7.1.6

Ramachandran, V. S., & Gregory, R. L. (1991). Perceptual filling in of artificially induced scotomas in human vision. *Nature*, *350*, 699–702. doi:10.1038/350699a0

Rubin, E. (1915). *Synsoplevede figurer:Studier i psykologisk Analyse* (Første Del.). [Visually perceived figures. Studies in psychological analysis (Part one)]. København: Gyldendalske Boghandel, Nordisk Forlag. [Copenhagen: Gyldendalske Bookstore, Nordic Publishing].

Schölvinck, M. L., & Rees, G. (2009). Attentional influences on the dynamics of motion-induced blindness. *Journal of Vision*, *9*, 38.1–9. doi:10.1167/9.1.38

Schölvinck, M. L., & Rees, G. (2010). Neural correlates of motion-induced blindness in the human brain. *Journal of Cognitive Neuroscience*, *22*, 1235–1243. doi:10.1162/jocn.2009.21262

Sobel, K. V., Gerrie, M. P., Poole, B. J., & Kane, M. J. (2007). Individual differences in working memory capacity and visual search: The roles of top-down and bottom-up processing. *Psychonomic Bulletin & Review*, *14*, 840–845. doi:10.3758/BF03194109

Sokoliuk, R., & VanRullen, R. (2013). The flickering wheel illusion: When α rhythms make a static wheel flicker. *The Journal of Neuroscience: The Official Journal of the Society for Neuroscience*, *33*, 13498–13504. doi:10.1523/JNEUROSCI.5647-12.2013

Spearman, C. E. (1904). ''General Intelligence,'' objectively determined and measured. *The American Journal of Psychology*, *15*, 201–292.

Srinivasan, R., Russell, D. P., Edelman, G. M., & Tononi, G. (1999). Increased synchronization of neuromagnetic responses during conscious perception. *The Journal of Neuroscience: The Official Journal of the Society for Neuroscience*, *19*, 5435–5448.

Tong, F., Meng, M., & Blake, R. (2006). Neural bases of binocular rivalry. *Trends in Cognitive Sciences*, *10*, 502–511. doi:10.1016/j.tics.2006.09.003

Troncoso, X. G., Macknik, S. L., & Martinez-Conde, S. (2008). Microsaccades counteract perceptual filling-in. *Journal of Vision*, *8*, 15.1–9. doi:10.1167/8.14.15

Troxler, I. P. V. (1804). Über das Verschwinden gegebener Gegenstände innerhalb unseres Gesichtskreises [On the disappearance of given objects from our visual field]. In J. Himly, & J. A. Schmidt (Eds.), Über das Verschwinden gegebener Gegenstände innerhalb unseres Gesichtskreises [On the disappearance of given objects from our visual field]. *Ophthalmologische Bibliothek*, *2*, 1–53.

Tschacher, W., Schuler, D., & Junghan, U. (2006). Reduced perception of the motion-induced blindness illusion in schizophrenia. *Schizophrenia Research*, *81*, 261–267. doi:10.1016/j.schres.2005.08.012

van Loon, A. M., Knapen, T., Scholte, H. S., St John-Saaltink, E., Donner, T. H., & Lamme, V. A. F. (2013). GABA shapes the dynamics of bistable perception. *Current Biology: CB*, *23*, 823–827. doi:10.1016/j.cub.2013.03.067

Wallis, T. S. A., & Arnold, D. H. (2009). Motion-induced blindness and motion streak suppression. *Current Biology: CB*, *19*, 325–329. doi:10.1016/j.cub.2008.12.053

Welchman, A. E., & Harris, J. M. (2000). The effects of dot density and motion coherence on perceptual fading of a target in noise. *Spatial Vision*, *14*, 45–58.

Wells, E. T., Leber, A. B., & Sparrow, J. E. (2011). The role of mask coherence in motion-induced blindness. *Perception*, *40*, 1503–1518.

Wetherill, G. B., & Levitt, H. (1965). Sequential estimation of points on a psychometric function. *The British Journal of Mathematical and Statistical Psychology*, *18*, 1–10.

Wilson, H. R., Blake, R., & Lee, S. H. (2001). Dynamics of travelling waves in visual perception. *Nature*, *412*, 907–910. doi:10.1038/35091066

Wiseman, R., Watt, C., Gilhooly, K., & Georgiou, G. (2011). Creativity and ease of ambiguous figural reversal. *British Journal of Psychology (London, England: 1953)*, *102*, 615–622. doi:10.1111/j.2044-8295.2011.02031.x

Yuval-Greenberg, S., Merriam, E. P., & Heeger, D. J. (2014). Spontaneous microsaccades reflect shifts in covert attention. *The Journal of Neuroscience: The Official Journal of the Society for Neuroscience*, *34*, 13693–13700. doi:10.1523/JNEUROSCI.0582-14.2014

Zaretskaya, N., Thielscher, A., Logothetis, N. K., & Bartels, A. (2010). Disrupting parietal function prolongs dominance durations in binocular rivalry. *Current Biology: CB*, *20*, 2106–2111. doi:10.1016/j.cub.2010.10.046

Zhou, Y. H., Gao, J. B., White, K. D., Merk, I., & Yao, K. (2004). Perceptual dominance time distributions in multistable visual perception. *Biological Cybernetics*, *90*, 256–263. doi:10.1007/s00422-004-0472-8.

Appendix

Representative participants were selected to demonstrate similar dynamics within individuals and variation between individuals with ''low'', ''middle,'' and ''high'' rates of disappearance in MIB, TE, and PFI (see Figure A1). The low rate of disappearances example is a participant whose numbers of disappearances for all three phenomena were in the first quartile of the population distribution. The high rate of disappearances example is a participant whose number of disappearances was in the fourth quartile of the distributions

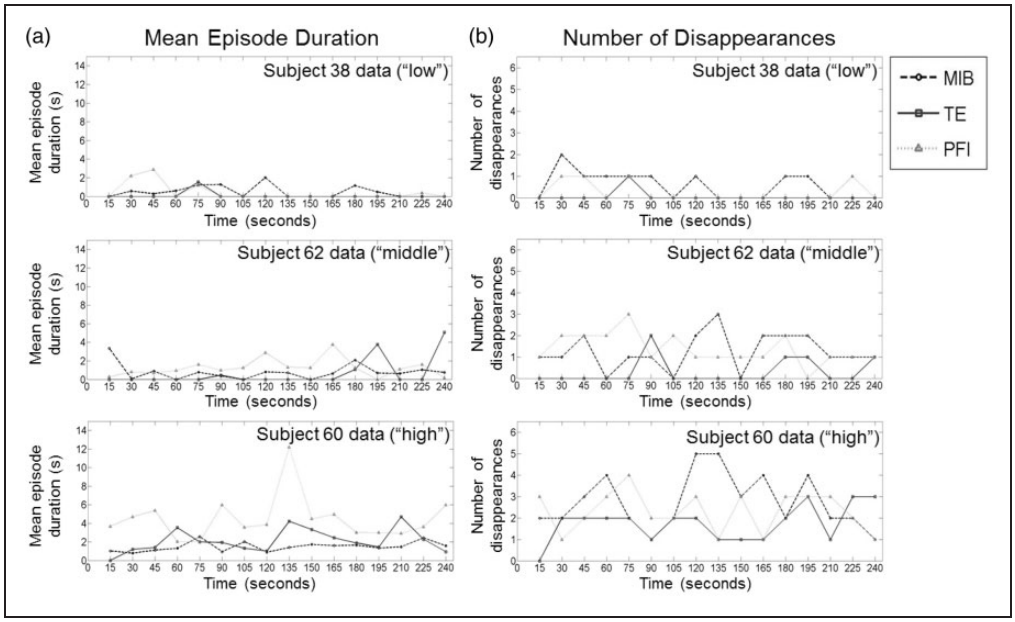

Figure A1. Time series data for three representative participants with low, middle, and high rates of disappearances for mean episode duration (left) and number of disappearances (right).

of total numbers of disappearances for all three phenomena. The middle rate of disappearances example is a participant whose numbers of disappearances for MIB and PFI were close to population median values and were between the 45th and 55th percentiles. This participant's total number of disappearances in TE fell within the first quartile of the corresponding distribution.